

## Optimum Feedback Controller Design for Tandem Cold Metal Rolling

John Pittner and Marwan A. Simaan

University of Pittsburgh, Department of Electrical and Computer Engineering,  
Pittsburgh, PA 15261 USA (Tel: 412-624-8099;  
e-mail: jpittner@engr.pitt.edu, simaan@engr.pitt.edu)

**Abstract:** Controlling the tandem cold rolling of metal strip is a significant challenge to the control engineer. This is due mostly to complex interactions between the process variables, nonlinearities that change with process conditions, and long speed-dependent time delays. The present technology is limited in its capability for improvement in performance. This paper describes a new control strategy that is based on solving a state-dependent algebraic Riccati equation pointwise to establish a control law for a MIMO controller that is augmented by appropriate trimming functions. Simulation testing showed that the tolerance in mill exit thickness compares favorably to the tolerances using existing techniques.

### 1. INTRODUCTION

A typical cold metal rolling process (Fig. 1) consists of five pairs of independently driven work rolls through which is passed a metal strip (e.g. steel), with each work roll supported by a back-up roll of larger diameter. As the strip passes through the individual pairs of work rolls, the thickness is successively reduced by very high compression stress in a small region (the roll bite) between the work rolls. Hydraulic rams or a screw arrangement driven by an electric motor provides the necessary compression force.

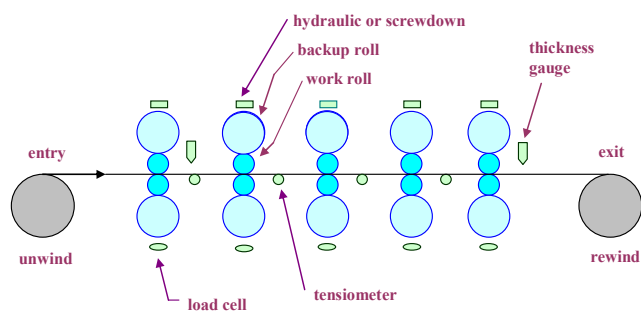


Fig. 1. Typical 5-stand tandem cold mill

The process is monitored by instrumentation which provides signals that represent the roll force at each stand, the interstand strip tension forces, the strip thickness at the exit of the first and last stands, the roll gap actuator (hydraulic ram or screw) positions, and the work roll speeds.

During threading the strip is successively introduced at low speed into the mill stands from a coil formed during previous processing. After the last stand is threaded and tension is established at the rewind, the speed is increased to the desired operating speed (i.e. run speed). The speed is lowered for de-threading when the unwind is nearly empty, which is followed by a setup of the mill for the next coil to be processed.

The current technology for control of tandem cold rolling generally consists of a control structure (Bryant, 1973) which decomposes the overall control problem into several separate sub-problems to attempt to provide the independent adjustment of strip tension and thickness everywhere in the mill. While this method and its variations (e.g. Carlton and Conway, 1992; Duval et al., 1991) are effective in producing an acceptable product, it is recognized that the application of other design techniques (e.g. Geddes and Postlewaite, 1998; Hoshino, 1998) might improve performance. However, many of these methods (e.g. Geddes and Postlewaite, 1998) have some limitations related to the complexity of the control implementation, the requirement for a linearized process model, the accommodation of changes in the mill speed and in the product being processed. This is especially significant in the case of the continuous process wherein the product characteristics change very rapidly on the fly during the passage of the weld which generally occurs at reduced speed.

We present in this paper an alternate control method which is based on a state-dependent algebraic Riccati equation technique that is implemented in a pointwise basis and augmented by appropriate trimming functions. Our objective is to build on our previous results (Pittner and Simaan, 2006, 2004) to fully develop this new method and investigate its theoretical and applied aspects. The evaluation of this method is based on two criteria which are considered significant in the control of the tandem cold mill: (1) Reducing the excursions in thickness and tension from their operating point values and (2) Simplicity in design and implementation.

### 2. THE PROCESS MODEL

The following expressions which comprise the process model are based on a series of well-known and well-verified algebraic equations developed for control purposes (Bryant, 1973). Stand  $i$  is understood where no subscript is given.

The specific roll force is approximated in the roll bite area of a mill stand as

$$P = (\bar{k} - \bar{\sigma}) \sqrt{R' \delta} (1 + 4\alpha), \quad (1)$$

where

$$\alpha = \sqrt{\frac{h_{out}}{h_{in}}} \exp\left(\frac{\mu \sqrt{R' \delta}}{\bar{h}}\right) - 1, \quad (2)$$

and  $P$  is the specific roll force,  $\bar{k}$  is the mean yield stress (hardness),  $\bar{\sigma}$  is the mean tension stress,  $R'$  is the deformed work roll radius,  $\delta$  is the draft, i.e.  $(h_{in} - h_{out})$ ,  $h_{in(out)}$  is the input (output) strip thickness,  $\bar{h}$  is the mean strip thickness, and  $\mu$  is the coefficient of friction.

The forward slip is the fractional increase in the speed of the strip exiting the roll bite area, with respect to the strip speed at the neutral plane. The forward slip is approximated by

$$f = \left(\frac{\delta}{h_{out}}\right) \left(\frac{\phi_n}{\phi_l}\right)^2, \quad (3)$$

where  $f$  is the forward slip, the angle at the neutral plane and the contact angle respectively are

$$\phi_n = \frac{1}{2} \frac{h_{out}}{\bar{h}} \sqrt{\frac{\delta}{R'}} - \frac{1}{4} \frac{h_{out} \delta}{\bar{h} \mu R'} + \frac{1}{4} \frac{h_{out}}{\mu R'} \left(\frac{\sigma_{out}}{k_{out}} - \frac{\sigma_{in}}{k_{in}}\right), \quad (4)$$

and

$$\phi_l = \sqrt{\frac{\delta}{R'}}, \quad (5)$$

with  $\sigma_{in(out)}$  the input (output) tension stress, and  $k_{in(out)}$  the input(output) compressive yield stress.

An expression for the interstand tension stress is obtained by applying Hooke's law to a length of strip between successive stands as

$$\frac{d\sigma_{i,i+1}}{dt} \equiv \dot{\sigma}_{i,i+1} = \frac{E(V_{in,i+1} - V_{out,i})}{L_0}, \quad \sigma_{i,i+1}(0) = \sigma_{0,i,i+1}, \quad (6)$$

where  $E$  is Young's modulus,  $V_{in(out)}$  are the input (output) strip speeds at a mill stand, and  $L_0$  is the distance between adjacent mill stands.

A linear approximation for the mill stretch characteristic is used to estimate the thickness at the exit of a stand as

$$h_{out} = S + SO + \frac{F}{M}, \quad (7)$$

where  $F = PW$  is the total roll force,  $W$  is the strip width,  $SO$  is the intercept of the linearized approximation, and  $M$  is the mill modulus.

The work roll actuator position controller and the work roll speed controller are modeled respectively based on typical mill data and experience

$$\dot{S} = \frac{U_S}{\tau_S} - \frac{S}{\tau_S}, \quad S(0) = S_0, \quad (8)$$

and

$$\dot{V} = \frac{U_V}{\tau_V} - \frac{V}{\tau_V}, \quad V(0) = V_0, \quad (9)$$

where  $S$  is the roll position actuator position,  $V$  is the work roll peripheral speed,  $U_S$  and  $U_V$  are the position and speed regulator references, and  $\tau_S$  and  $\tau_V$  are the associated time constants.

The interstand time delay is approximated at any instant of time as

$$\tau_{d,i,i+1} = \frac{L_0}{V_{out,i}}. \quad (10)$$

The input thickness, mean yield stress, mean tension stress, mean thickness, friction coefficient, deformed work roll radius, draft, stand output strip speed, and stand input strip speed are modeled as in Pittner (2006). The above relationships are put into a state-space model as described by (11) and (12). Relationships which express  $P$ ,  $h_{out}$ , and  $(V_{in,i+1} - V_{out,i})$ , as functions of the state variables are derived also as shown in Pittner (2006).

The above expressions are put into the form of a state equation (11) and an output equation (12),

$$\dot{x} = a(x) + Bu, \quad x(0) = x_0, \quad (11)$$

$$y = g(x), \quad (12)$$

where  $x \in R^n$ ,  $y \in R^p$ ,  $u \in R^m$ , are vectors whose elements represent the individual state variables, output variables, and control variables respectively,  $a(x) \in R^n$  and  $g(x) \in R^p$  are state-dependent vectors, and  $B \in R^{n \times m}$  is a constant matrix.

The state variables, control variables, and output variables represented by the elements of the vectors  $x$ ,  $u$ , and  $y$  respectively in (11) and (12) are as shown in Table 1, where, with  $i$  representing the stand number,  $\sigma_{i,i+1}$  is the interstand tension stress,  $S_i$  is the roll gap actuator position,  $V_i$  is the work roll linear speed,  $U_{Si}$  is the roll gap actuator position reference,  $U_{Vi}$  is the work roll drive speed reference,  $h_{out,i}$  is the output thickness, and  $P_i$  is the specific roll force.

**Table 1. Variable Assignments: State Vector, Output Vector, and Control Vector**

State Vector		Control Vector		Output Vector	
$x_1 (\sigma_{12})$	$x_8 (S_1)$	$u_1 (U_{S1})$	$u_6 (U_{V1})$	$y_1 (h_{out1})$	$y_8 (\sigma_{34})$
$x_2 (\sigma_{23})$	$x_9 (S_2)$	$u_2 (U_{S2})$	$u_7 (U_{V2})$	$y_2 (h_{out2})$	$y_9 (\sigma_{45})$
$x_3 (\sigma_{34})$	$x_{10} (V_1)$	$u_3 (U_{S3})$	$u_8 (U_{V3})$	$y_3 (h_{out3})$	$y_{10} (P_1)$
$x_4 (\sigma_{45})$	$x_{11} (V_2)$	$u_4 (U_{S4})$	$u_9 (U_{V4})$	$y_4 (h_{out4})$	$y_{11} (P_2)$
$x_5 (S_1)$	$x_{12} (V_3)$	$u_5 (U_{S5})$	$u_{10} (U_{V5})$	$y_5 (h_{out5})$	$y_{12} (P_3)$
$x_6 (S_2)$	$x_{13} (V_4)$			$y_6 (\sigma_{12})$	$y_{13} (P_4)$
$x_7 (S_3)$	$x_{14} (V_5)$			$y_7 (\sigma_{23})$	$y_{14} (P_5)$

The model described by (11) and (12) was verified (Pittner, 2006) by open loop simulations which in general showed good consistency with results of Bryant (1973) and Geddes (1998).

### 3. THE CONTROLLER

The controller is based on the state-dependent Riccati equation (SDRE) technique (Clautier, 2002, 1996) which is similar to the well-established LQR method (Athans and

Falb, 1966) except that the coefficient matrices in the state and output equations and the control and state weighting matrices are state dependent. This method is developed by expressing the nonlinear plant dynamics in the form

$$\dot{x} = a(x) + b(x)u, \quad x(0) = x_0, \quad (13)$$

$$y = g(x). \quad (14)$$

By factorizing the state-dependent vectors and with  $b(x)=B$ , the above becomes a form resembling linear state space equations

$$\dot{x} = A(x)x + Bu, \quad x(0) = x_0, \quad (15)$$

$$y = C(x)x, \quad (16)$$

where  $A(x) \in R^{n \times n}$  and  $C(x) \in R^{p \times n}$  are state-dependent matrices, with  $x, u, y$ , and  $B$  as noted previously. It is known (Clautier, 2002) that, with  $a(0) = 0$ , and if  $a(x) \in C^l$ , an infinite number of such factorizations exist, and similarly with  $g(x)$ . The optimal control problem is to minimize the performance index

$$J = \frac{1}{2} \int_0^{\infty} (x'Q(x)x + u'R(x)u) dt \quad (17)$$

with respect to the control vector  $u$ , subject to the constraint (15), where  $Q(x) \geq 0$ ,  $R(x) > 0$ ,  $a(x) \in C^k$ ,  $R(x) \in C^k$ , for  $k \geq 1$ . The objective (17) is to find a control law which regulates the system to the origin, with the assumptions  $a(0)=0$ , and  $B \neq 0$ . The method of solution is first to factorize  $a(x)$  such that (13) can be expressed in the form of (15). The state-dependent algebraic Riccati equation

$$A'(x)K(x) + K(x)A(x) - K(x)BR^{-1}(x)B'K(x) + Q(x) = 0 \quad (18)$$

then is solved pointwise for  $K(x)$ , which results in the control law

$$u = -R^{-1}(x)B'K(x)x. \quad (19)$$

Assuming the availability of full state measurement, the method requires that the pair  $(A(x), B)$  be pointwise stabilizable (in a linear sense) for all  $x$  in the control space in order to ensure a solution to (18) at each point. Local asymptotic stability is assured (Clautier, 1996) if  $(A(x), B)$  is pointwise stabilizable, if there exists a matrix  $C_l(x)$  such that  $Q(x) = C_l'(x)C_l(x)$ , and if  $(A(x), C_l(x))$  is pointwise detectable, assuming that  $A(x) \in C^k$ . Global asymptotic stability must be confirmed by simulation since, except for special cases (Erdem, 2001) there is no known useful theory which guarantees it.

In the case of the SDRE method the necessary condition for the optimal control problem usually is not satisfied. However if each element of  $A(x)$ ,  $K(x)$ ,  $Q(x)$ ,  $R(x)$ , and each element of their partial derivatives  $A_x(x)$ ,  $K_x(x)$ ,  $Q_x(x)$ ,  $R_x(x)$ , is bounded for all  $x$  in the control space, and under global asymptotic stability, then the state trajectories converge to the optimal state trajectories as the states are driven to zero, which is taken to be a suboptimal condition (Clautier, 1996).

### 3.1 Application to Tandem Cold Rolling

The simplicity of the SDRE method and its capability to improve physical intuition in the design process make it quite desirable. However, it should be noted that the application of this technique must rely heavily on physical intuition and simulation to develop and confirm a controller design, with the individual controller parameters being set intuitively and confirmed by simulation.

An operating point for the tandem cold mill is determined by the product being rolled and the desired mill speed. An objective of the controller is that excursions (from the operating point) in the exit thickness and in the interstand tension stresses be as low as reasonably achievable in the presence of external and internal disturbances, and with uncertainties in modelling and measurements. In addition, the operator must have the capability to independently adjust the stand exit thicknesses and the interstand tensions during the actual rolling process.

The typical significant external disturbances are excursions in mill entry thickness and mill entry hardness as shown in Fig. 2. The significant internal disturbances, which are addressed in Section 3.3, are eccentricity effects in the rolls of the tandem cold mill. The uncertainties considered are those in the measurement of process parameters (Table 2), and those in modeling (Table 3) where the listed estimated uncertainties are percentages of the measured values except for  $F$ ,  $\sigma$ , and  $S$  which are percentages of full scale values. For consistency with data reported from operating mills, the estimated uncertainty for  $h_{out1m(5m)}$  is taken to be zero.

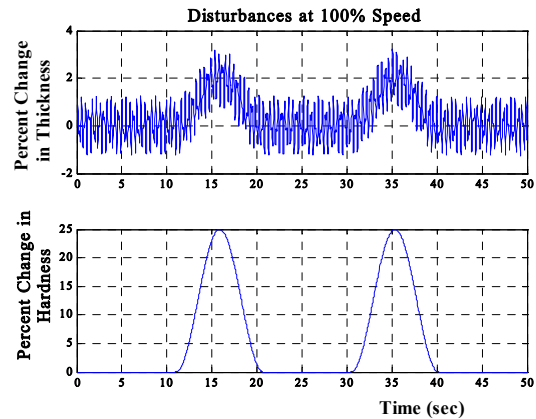


Fig. 2. Typical mill entry disturbances

Table 2. Measurement Uncertainties

Parameter	Estimated Uncertainty	Source of Estimate
$h_{out1m(5m)}$	0%	n/a
$F$	0.2%	Roberts, 1987
$\sigma$	0.2%	Ginzburg, 1993
$S$	0.05%	ibid.
$V$	0.05%	ibid.
$V_{in,2,3,4,5}$	0.025%	Zillman, 2004.
$V_{out5}$	0.025%	ibid.

**Table 3. Modelling Uncertainties**

Parameter	Estimated Uncertainty	Source of Estimate
$\mu$	20%	Roberts, 1978
$M$	10%	Teoh, 1984
$k$	25%	experience

3.2 Structure of the Controller

The controller structure is depicted in Fig. 3. In Fig. 3 the effects of disturbances and uncertainties are modeled separately but are depicted as shown for simplicity of presentation. The vectors  $x$ ,  $u$ , and  $y$  at the operating point are represented as  $x_{op}$ ,  $u_{op}$ , and  $y_{op}$ . A coordinate change is performed by the introduction of the vector  $z=x-x_{op}$  which shifts the operating point to the origin. The performance index (17) is then modified to be

$$J = \frac{1}{2} \int_0^{\infty} (z' Q z + (u - u_{op})' R (u - u_{op})) dt, \quad (20)$$

where for simplicity  $Q$  and  $R$  are diagonal matrices with tunable constant elements. A change in mill speed is effected by changing the operating point, which is done by changing the variables corresponding to the elements of  $x_{op,i}$  ( $i=10, \dots, 14$ ) and of  $u_{op,i}$  ( $i=6, \dots, 10$ ) (Table 1) proportionally to a mill master speed reference.

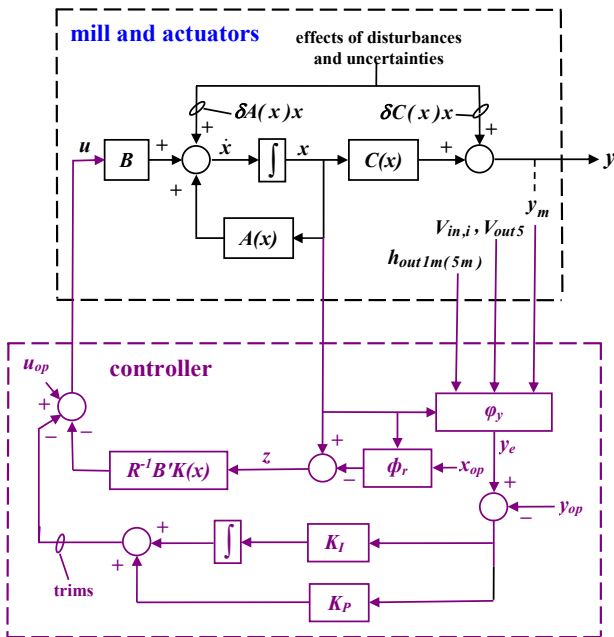


Fig. 3 Controller coupled to model of mill and actuators

The SDR controller is the basic MIMO control for the mill. The control of each stand output thickness is enhanced by a PI trim function to achieve zero steady-state error. This also greatly reduces the effect of the interstand time delay by providing a fast-responding trim loop which does not include the time delay. The strip speeds at the inputs to stands 2, 3, 4, 5, and at the output of stand 5 are measured by high accuracy velocimeters. The measured strip speed signals are used for the estimation of strip thicknesses at the outputs of stands 2

through 5 using mass flow techniques, and for tracking strip thickness through the mill.

A trim function (Fig. 4) corrects for slight offsets in the interstand tensions from the operating point values for each interstand tension. The final control of the tensions is achieved by the control law that is computed pointwise by the SDR controller to provide signals to the work roll actuator position controllers and the work roll speed controllers so that excursions in the tensions are reduced, which is essential for the stability of rolling.

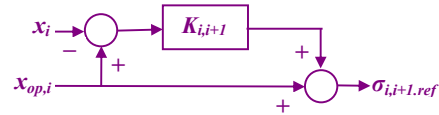


Fig. 4. Interstand tension operating point trim

The algorithm  $\phi_r$  in Fig. 3 represents interstand tension operating point trims which are implemented as shown in Fig. 4 where  $x_{op,i}$  ( $i=1,2,3,4$ ) is an element of the vector  $x_{op}$  that represents the operating point for the interstand tension for stands  $i,i+1$ ,  $\sigma_{i,i+1,ref}$  is the interstand tension reference for stands  $i,i+1$ ,  $x_i$  is the element of the state vector which represents the measured interstand tension for stands  $i,i+1$ , and  $K_{i,i+1}$  is a gain term for stands  $i,i+1$ . A direct feed-through is provided for elements  $x_{op,i}$  ( $i=5, \dots, 14$ ).

In the controller (Fig. 3), each element of the state vector  $x$  is measurable,  $y_m$  represents the measurable elements of the output vector  $y$ ,  $y_e \in R^p$  ( $p=14$ ) is a vector whose elements are the measured (or estimated) elements of  $y$ ,  $\phi_y$  is an algorithm which generates  $y_e$ ,  $V_{in,i}$  ( $i=2,3,4,5$ ) and  $V_{out5}$  are the measured strip speeds at the inputs of stands 2, 3, 4, 5, and at the output of stand 5,  $h_{out1(5)m}$  are the measured output thicknesses at stands 1 and 5,  $K_p \in R^{m \times p}$  and  $K_i \in R^{m \times p}$  ( $m=10, p=14$ ) are matrices whose elements are zero except for elements  $(j, j)$ , ( $j = 1,2,3,4,5$ ), which are the gains for the thickness trim functions.

An estimate of  $h_{out1}(y_1)$  is computed by the algorithm  $\phi_y$  as shown in Fig. 5, with  $h_{out1b}$  determined using the estimate,

$$h_{out1b} = x_5 + S0 + \frac{F1}{M1e}, \quad (21)$$

where the notation  $h_{out1e}(y_{1e})$  indicates that the variable  $h_{out1e}$  is represented by element 1 of vector  $y_e$ .

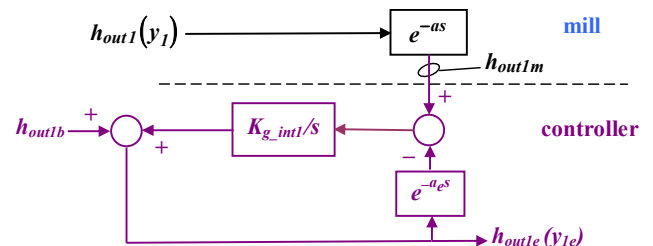


Fig. 5. Stand 1 output thickness estimation

A nearly immediate response in the estimated output

thickness  $h_{out1e}(y_{1e})$  is provided by the configuration of Fig. 5. The undesirable effects of the time delay between the strip thickness at the exit of stand 1 and the thickness gauge downstream of stand 1 are mitigated by using (21) to provide this response. The effects of roll eccentricity and the uncertainty in  $M_{1e}$  on the estimated  $h_{out1b}$  are quite small as shown later in this section and in Section 4.

The estimated thickness  $h_{out2e}(y_{2e})$  is computed as

$$h_{out2e} = \frac{V_{in2}}{V_{in3}} h_{in2e} k_{2e}, \quad (22)$$

where  $h_{in2e}$  is  $h_{out1m}$  as tracked from the thickness gauge to stand 2, and  $k_{2e}$  is a correction factor as noted in what follows. Estimates of thicknesses  $h_{out3e}(y_{3e})$  and  $h_{out4e}(y_{4e})$  are determined similarly, except that tracking is from the previous stand.

The output thickness for stand 5 is determined as

$$h_{out5b} = \frac{V_{in5}}{V_{out5}} h_{in5e} k_{5e}, \quad (23)$$

where  $h_{in5e}$  is  $h_{out4e}(y_{4e})$  as tracked from stand 4 to stand 5, and  $k_{5e}$  is a correction factor similar to  $k_{2e}$ . The control of output thickness is similar to stand 1 except that a mass flow technique (23) is used to provide a nearly immediate response in the estimated output thickness  $h_{out5e}(y_{5e})$ . The factors  $k_{ie}$  ( $i=2,3,4,5$ ), which are used in the estimation of strip thicknesses  $h_{out2e}$ ,  $h_{out3e}$ ,  $h_{out4e}$ , and  $h_{out5b}$  to correct for small errors (such as spreading, reductions in width, or other effects), are set during operation by a separate mill adaptation system.

An attenuation of steady-state errors in the stand output thicknesses resulting from the uncertainties of Tables 2 and 3 occurs since the uncertainties are inside the closed loops of the thickness trims (Fig. 3). An exception is the errors caused by the uncertainties in the measurements of  $V_{in,i}$  ( $i=2,3,4$ ) that are used in the computation of  $h_{out,i,e}$  for stands 2,3,4, e. g. (22). These errors are small since the uncertainties in the measurement of  $V_{in,i}$  are small. Transient errors in thicknesses due to uncertainties also are small because any changes in the thickness trim control loops, or the errors themselves are small. In the case of stand 1, where the estimate (21) is used, the estimate of  $h_{out1b}$  is sensitive to the uncertainty in  $M_{1e}$ . To reduce the effects of this uncertainty, a mill modulus  $M_I$  is computed using (7) and measurements of  $h_{out1m}$ ,  $F_I$ , and  $S_I$ , where the measurements of  $F_I$  and  $S_I$  are delayed by the time delay from stand 1 to the thickness gauge. The estimated mill modulus  $M_{1e}$  is then taken to be equal to  $M_I$  since changes in  $M_I$  are slow compared to the time delay.

Independent adjustment of the stand output thicknesses and the interstand tension stresses is effected simply by changing the variables represented by the elements of the vector  $y_{op,i}$  ( $i=1, \dots, 5$ ) and the elements of the vector  $x_{op,i}$  ( $i=1, \dots, 4$ ), respectively (Table 1). Simulation, which confirmed the independence of adjustment, showed that an adjustment of 2% in a stand output thickness, or an adjustment of 5% in an interstand tension, resulted in a negligible effect on the

unadjusted interstand tensions and on the unadjusted steady-state stand output thicknesses.

### 3.3 Eccentricity Compensation

In general roll eccentricity is an axial deviation between the roll barrel and the roll neck caused by irregularities in the mill rolls, in the roll bearings, or in both, which results in cyclic variations in the strip thickness. In the model, roll eccentricity modifies (7) as

$$h_{out} = S + S0 + \frac{F}{M} + e, \quad (24)$$

where  $e$  is the roll eccentricity.

Mitigation of the effects of roll eccentricity is separate from the controller. However, it must be considered to be consistent with data reported from operating mills which usually includes eccentricity effects. The eccentricity components remaining in the mill exit thickness after compensation have been estimated by simulation using the method described in the following section.

## 4. SIMULATIONS

MATLAB/Simulink simulations (closed-loop) were performed for six different operating points with the controller (Fig. 3) coupled to the model and using the mill and strip properties of Bryant (1973). Presentation of the complete simulation results (Pittner 2006) are precluded by restrictions on the paper length. The results presented are for the operating point of Table 4 and are typical for the other operating points. Total compensation of eccentricity was assumed initially to highlight the performance of the controller.

**Table 4. Typical Operating Point**

Mill Entry Thickness	3.56 mm (0.140 in)
Exit Thickness, Stand 1	2.95 (0.116)
Exit Thickness, Stand 2	2.44 (0.096)
Exit Thickness, Stand 3	2.01 (0.079)
Exit Thickness, Stand 4	1.67 (0.066)
Exit Thickness, Stand 5	1.58 (0.062)
Tension Stress, Mill Entry	0.0 Kg/mm <sup>2</sup> (0.0 tons/in <sup>2</sup> )
Tension Stress, Stands 1,2	8.9 (5.6)
Tension Stress, Stands 2,3	9.0 (5.7)
Tension Stress, Stands 3,4	9.1 (5.8)
Tension Stress, Stands 4,5	9.4 (6.0)
Tension Stress, Mill Exit	2.8 (1.8)

With the mill entry disturbances applied and with uncertainties the maximum percent deviations of the stand exit thicknesses and of the interstand tension stress were less than 0.08% and 0.2% respectively, during operation at steady speed and during speed change. For each case simulated the uncertainties and the disturbances were applied concurrently and in a manner (determined intuitively and with a few trials)

that produced the maximum credible excursion in the mill exit thickness.

Simulation of the internal disturbances was done by assuming a cold mill roll eccentricity of 0.0305 mm (0.0012 inches) (Geddes, 1978), with eccentricity occurring only in the backup rolls, the backup rolls being identical, and assuming an active method of compensation by an adaptive noise cancellation technique using the measured speed of a work roll (Pittner, 2006). The resulting eccentricity component in the mill exit thickness was less than 0.05%.

An excursion of 0.2% (maximum) in the mill exit thickness was determined by adding the maximum excursion in stand 5 exit thickness (0.08%) to the eccentricity component (0.05%), plus 0.07% as a "safety margin" to allow for margins in the estimates of disturbances and uncertainties. Thus the new controller offers the potential for improvement over typical data reported from two well-performing industrial controllers denoted in Table 5 as mill A (Tezuka et al., 2001) and mill B (Sekiguchi et al., 1996). In addition, the reduced excursions in the output thickness and in the interstand tensions strongly contribute to the stability of the rolling process.

**Table 5. Comparison with Controllers for Mill A and Mill B**

Controller	Magnitude of Maximum Percent Deviation of Mill Exit Thickness
SDRE-Based	.2%
Mill A	.5
Mill B	.8

## 5. CONCLUSION

In addition to the benefits noted herein, the new technique appears to be especially useful for a continuous mill where the speed is changed for weld passage and the product characteristics change quite rapidly on the fly. This conclusion is based on the results of our recent work (Pittner and Simaan, 2007) involving the control of continuous mills. Further, the possibility for expansion of the new technique to improve the control of strip shape, flatness in particular, is recommended as an important issue for future investigation.

## ACKNOWLEDGEMENT

This work was supported in part by a grant from the Pennsylvania Infrastructure Technology Alliance (PITA).

## REFERENCES

Athans, M. and P.L. Falb (1966). *Optimal control an introduction to the theory and its applications*, Chap. 9. McGraw-Hill, New York,.

Bryant, C.F. (1973). *Automation of tandem mills*, British Iron and Steel Institute, London, UK.

Carlton, A.J. and R.G. Conway (1992). Automation of the LTV steel Hennepin tandem cold mill. *Iron and steel engineer*, pp. 17-28.

Clautier, J.R. and D.T. Stansbery (2002). The capabilities and art of state-dependent Riccati equation-based design,

*Proceedings of the american control conference*, pp. 86-91. Anchorage, Alaska.

Clautier, J.R., N. D'Souza and C.P. Mracek (1996). Nonlinear regulation and nonlinear  $H^\infty$  control via the state-dependent Riccati equation technique: part I, theory, *Proceedings of the international conference on nonlinear problems in aviation and aerospace*, Embry Riddle University, pp. 117-131.

Duval, P., J.C. Parks and G. Fellus (1991). Latest AGC technology installed at LTV's Cleveland 5-stand cold mill. *Iron and steel eng'r*, pp. 46-51.

Erdem, E.B. (2001). *Analysis and real-time implementation of state-dependent Riccati equation controlled systems*, PhD Thesis, University of Illinois, Urbana-Champaign.

Geddes, E.J.M. (1998). *Tandem cold rolling and robust multivariable control*, PhD thesis, University of Leicester, UK.

Geddes, E.J.M. and I. Postlewaite (1998). Improvements in product quality in tandem cold rolling using robust multivariable control. *IEEE trans on control systems tech.*, **6** (2), pp. 257-269.

Ginzburg, V.B. (1993). *High quality steel rolling, theory and practice*, Chap. 9. Marcel-Dekker, New York,.

Hoshino, I. et al. (1998). Observer-based multivariable control of the aluminum cold tandem mill, *Automatica*, **24** (6), pp.741-754.

Pittner, J.R. and M.A. Simaan (2007). A novel approach for optimal control of continuous tandem cold metal rolling, *Conference record of the 42<sup>nd</sup> IEEE industry applications society 2007 annual Meeting*, New Orleans, Louisiana.

Pittner, J.R. (2006). *Pointwise linear quadratic optimal control of a tandem cold rolling mill*, PhD Thesis, University of Pittsburgh, Pittsburgh.

Pittner, J.R. and M.A. Simaan (2006). State-dependent Riccati equation approach for optimal control of a tandem cold metal rolling process, *IEEE transactions on industry applications*, **42** (3), pp. 836-843.

Pittner, J.R. and M.A. Simaan (2004). Pointwise linear quadratic optimal control of a tandem cold rolling mill, *Conference record of the 39<sup>th</sup> IEEE industry application society 2004 annual meeting*, pp. 903-910, Seattle, Washington.

Roberts, W.L. (1987). *Flat processing of steel*, Chap.14,22. Marcel Dekker, New York.

Roberts, W. L. (1978). *Cold rolling of steel*, Chap. 6. Marcel Dekker, New York.

Sekiguchi, K. et al. (1996). The advanced set-up and control system for Dofasco's tandem cold mill, *IEEE transactions on industry applications*, **32** (3), pp. 608-616.

Teoh, E.K. et al. (1984). An improved thickness controller for a rolling mill, *Proceedings of IFAC 9<sup>th</sup> triennial world congress*, pp. 1741-1746. Budapest, Hungary,

Tezuka, T. et al. (2001). Application of a new automatic gauge control system for the tandem cold mill, *IEEE IAS 2001 conference record of the 36<sup>th</sup> IAS annual meeting*, **2**, pp. 955-960.

Zillman, M. (2004). Accuspeed laser velocimeter model ASD1000A description and spec DS.ASPD.808.2, *George Kelk Corp. US-7196Q*.